

Support information

HKUST-1 Loaded Few-layer $\text{Ti}_3\text{C}_2\text{T}_x$ for Synergistic Chemo-Photothermal Effects to Enhance Antibacterial Activity

Lei Fang^{†,a}, Yingjie Chen^{†,a}, Wei Shan^a, Tiankun Hui^a, Ilham Mokni^c, Jie Wu^c, Chuanli Zhou^{*,b},
Liangmin Yu^{*,a}, Meng Qiu^{*,a}

^a Key Laboratory of Marine Chemistry Theory and Technology (Ocean University of China), Ministry of Education, Qingdao 266100, China

^b Department of Spine Surgery, Affiliated Hospital of Qingdao University, Qingdao, Shandong, P. R. China

^c Department of Medicine, Zhejiang Chinese Medical University, Hangzhou, Zhejiang, China.

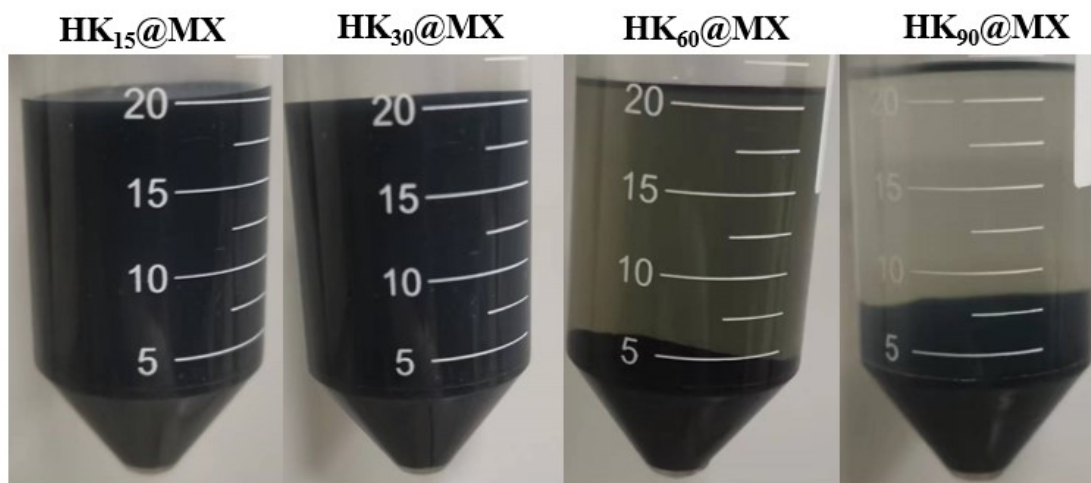


Figure S1 After the synthesis reaction, HK₁₅@MX, HK₃₀@MX, HK₆₀@MX and HK₉₀@MX were centrifuged in 2000 rpm/min for 5 minutes. The supernatant is getting cleaner while increase the loading of HKUST-1 on the surface of Ti₃C₂T_x. The high content of HKUST-1 on the surface of Ti₃C₂T_x leads to the mass increase and deposition to the bottom.

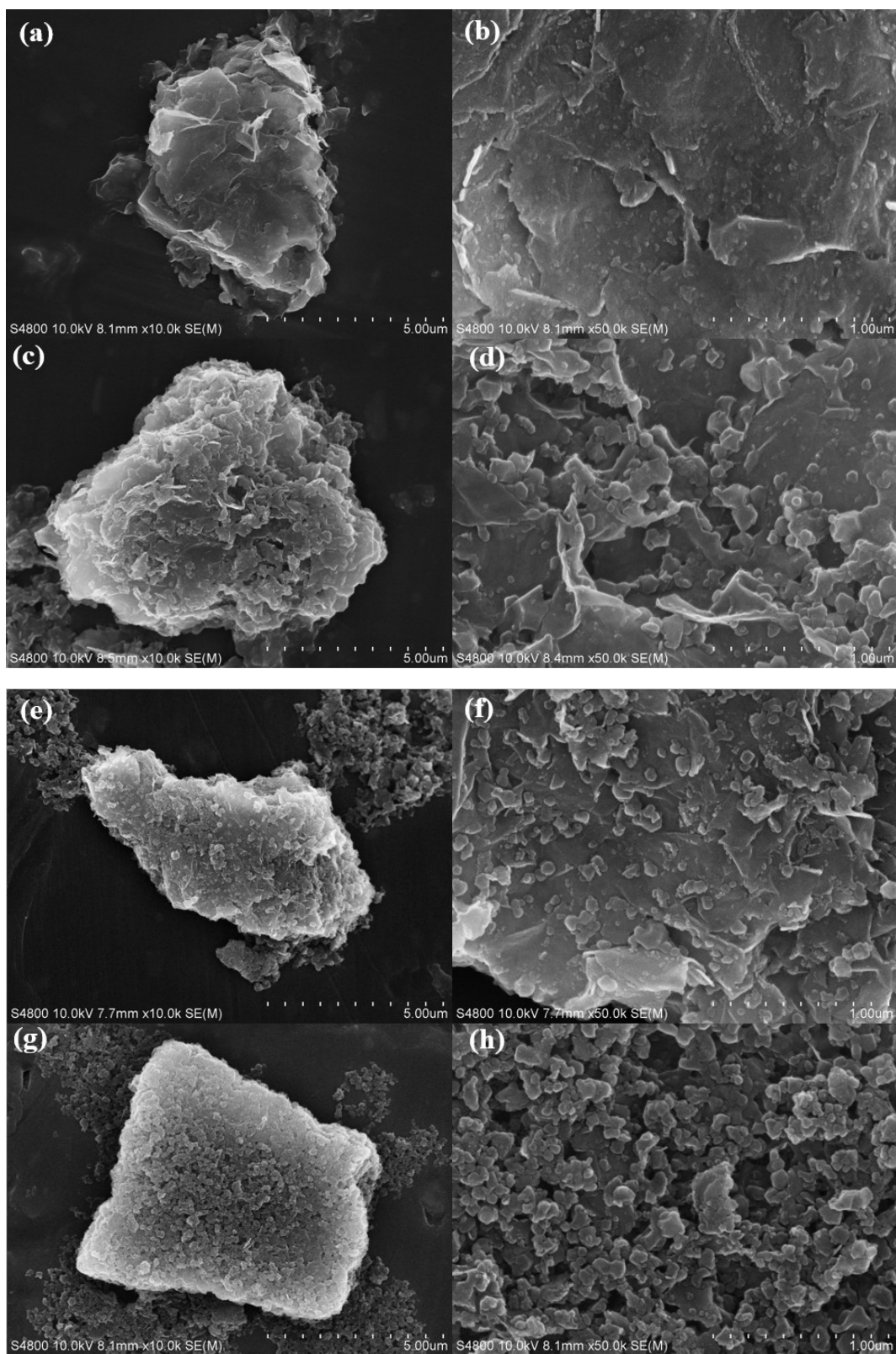
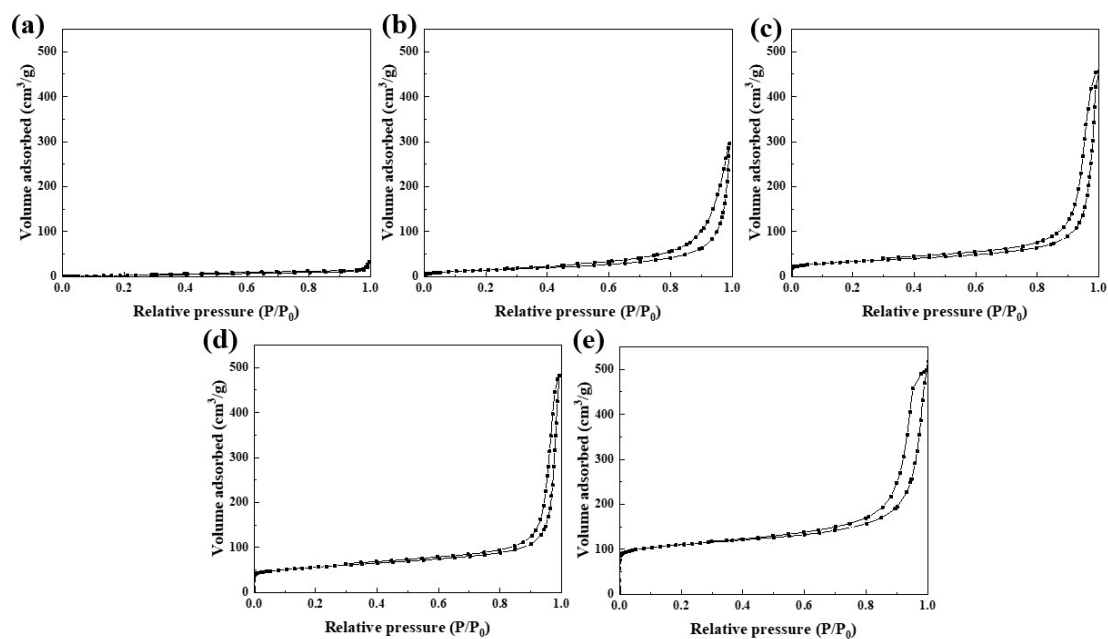


Figure S2. SEM images of (a-b) HK₁₅@Ti₃C₂T_x, (c-d) HK₃₀@Ti₃C₂T_x, (e-f) HK₆₀@Ti₃C₂T_x, (g-h) HK₉₀@Ti₃C₂T_x.

Table S1 Comparison of specific surface area and pore volume of $\text{Ti}_3\text{C}_2\text{T}_x$ and HK@MX samples

Materials	BET Surface Area ($\text{m}^2\cdot\text{g}^{-1}$)	Pore volume ($\text{cm}^3\cdot\text{g}^{-1}$)
$\text{Ti}_3\text{C}_2\text{T}_x$	11.748	2.68
$\text{HK}_{15}\text{@MX}$	57.226	13.157
$\text{HK}_{30}\text{@MX}$	109.45	25.149
$\text{HK}_{60}\text{@MX}$	131.03	30.105
$\text{HK}_{90}\text{@MX}$	186.76	42.908

**Figure S3** Nitrogen adsorption–desorption isotherms of (a) $\text{Ti}_3\text{C}_2\text{T}_x$, (b) $\text{HK}_{15}\text{@Ti}_3\text{C}_2\text{T}_x$, (c) $\text{HK}_{30}\text{@Ti}_3\text{C}_2\text{T}_x$, (d) $\text{HK}_{60}\text{@Ti}_3\text{C}_2\text{T}_x$, and (e) $\text{HK}_{90}\text{@Ti}_3\text{C}_2\text{T}_x$.

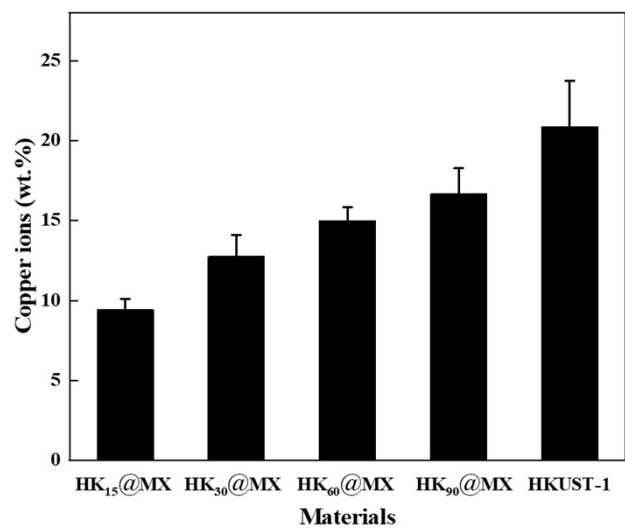


Figure. S4. ICP-MS analysis of Cu content in HKUST-1, HK₁₅@MX, HK₃₀@MX, HK₆₀@MX and HK₉₀@MX. (Calculation formula for measuring Cu element content= instrument reading × dilution factor × constant volume / sample quality. 10000 mg/kg = 1%.)

Photothermal performance of HK@MX

To evaluate the photothermal properties, a near-infrared laser (808 nm, 2 W cm⁻²) was used to irradiate deionized water and HK@MX nanoparticles at different concentrations for 10 minutes. Dispersion temperature was monitored by a type K thermocouple (OMEGA HH309A, OMEGA Engineering Inc., Norwalk, CT, USA). To calculate the photothermal conversion efficiency of HK@MX nanoparticles, 2 mL HK@MX nanoparticle aqueous dispersion (200 μg mL⁻¹) was irradiated continuously under the same conditions until the steady-state temperature was reached. Turn off the laser and record the temperature drop process. The photothermal conversion efficiency (η) is calculated by equation (1) described by literature¹:

$$\eta = \frac{hS(T_{max} - T_{surr}) - Q_s}{I(1 - 10^{-A_{808}})} \quad (1)$$

Where, h is the heat transfer coefficient, S is the surface area of the container, T_{max} is the maximum system temperature, T_{surr} is the ambient temperature, Q_s is the heat related to the optical absorbance of the solvent, I is the laser power (2 W cm⁻²), and A_{808} is the absorbance at HK₆₀@MX at 808 nm. The value of hS is derived from equation (2)

$$\tau_s = \frac{m_D C_D}{hS} \quad (2)$$

Including τ_s for sample system time constant, m_D and C_D respectively deionized water (1 g), and the quality of the heat capacity (4.2 J (g °C)⁻¹). The Q_s value measured independently using pure water was 13.4 mW.

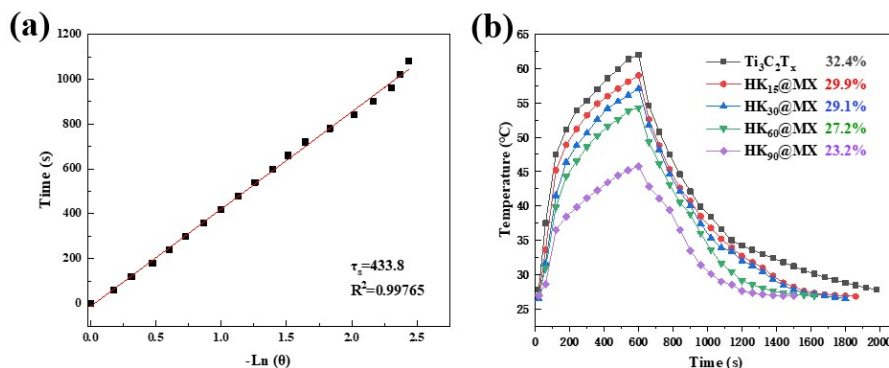


Figure. S5. (a) The fitting linear curve of time data vs $-\ln\theta$ from the cooling period of HK₆₀@MX. (b) The

heating/cooling curves of different nanoparticles with different HKUST-1 doping concentration under laser on/off.

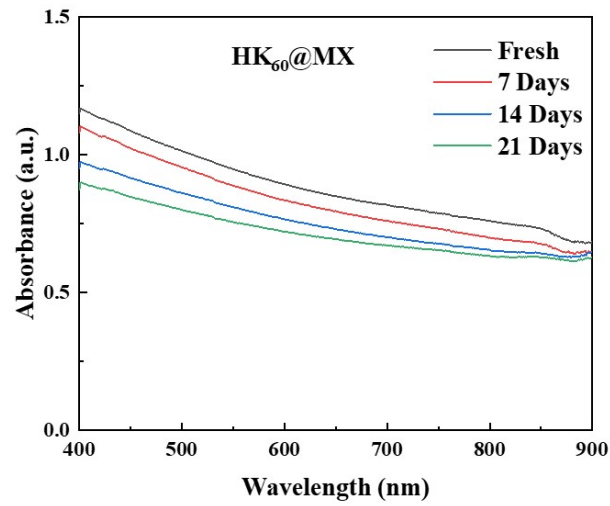


Figure. S6. Absorbance change of HK₆₀@MX dispersions in DI water for 21 days.

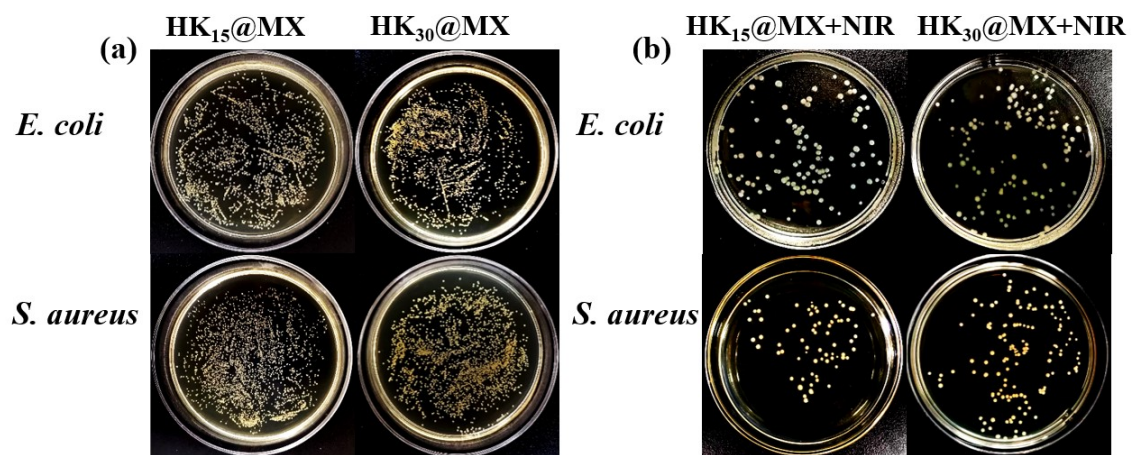
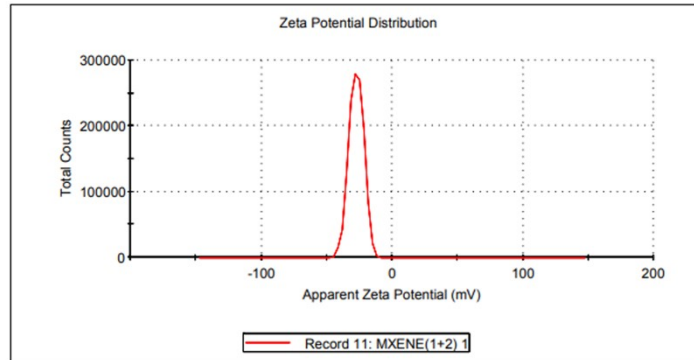


Figure S7 In vitro antibacterial activities of HK₁₅@MX and HK₃₀@MX against *S. aureus* and *E. coli*. (a) kept in the dark for 10 min (200 µg/ml) (b)exposed to 808 nm light (2 W/cm²) for 10 min

(a) Results

	Mean (mV)	Area (%)	St Dev (mV)
Zeta Potential (mV): -27.3	Peak 1: -27.3	100.0	5.53
Zeta Deviation (mV): 5.53	Peak 2: 0.00	0.0	0.00
Conductivity (mS/cm): 0.0250	Peak 3: 0.00	0.0	0.00

Result quality Good



(b) Results

	Mean (mV)	Area (%)	St Dev (mV)
Zeta Potential (mV): -4.46	Peak 1: -4.46	100.0	6.97
Zeta Deviation (mV): 6.97	Peak 2: 0.00	0.0	0.00
Conductivity (mS/cm): 0.0921	Peak 3: 0.00	0.0	0.00

Result quality Good

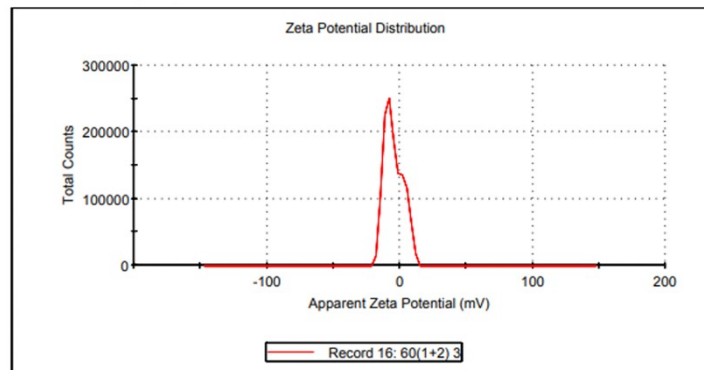


Figure S8 Distribution of zeta potential of (a) $\text{Ti}_3\text{C}_2\text{T}_x$ and (b) $\text{HK}_{60}\text{@MX}$ at pH 7.5

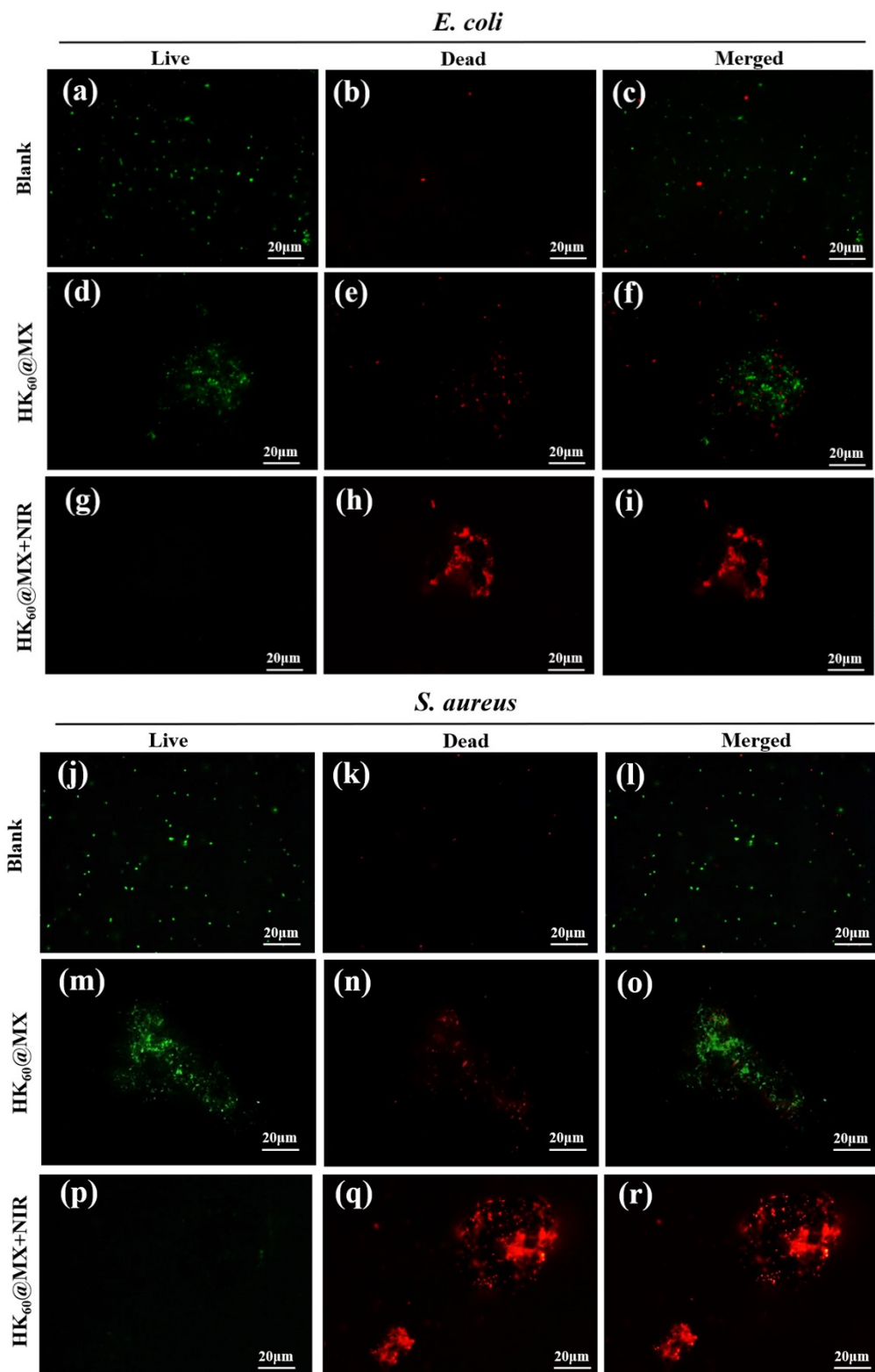


Figure S9. Confocal laser scanning microscopy (CLSM) images of *E. coli* (a-i) and *S. aureus* (j-r) treated with Meilungreen and PI staining. (a-c, j-l) control; (d-f, m-o) 200 $\mu\text{g}/\text{mL}$ HK₆₀@MX; (g-i, p-r) 200 $\mu\text{g}/\text{mL}$ HK₆₀@MX+NIR.

Notes and references

1. Z. Chu, T. Tian, Z. Tao, J. Yang, B. Chen, H. Chen, W. Wang, P. Yin, X. Xia, H. Wang and H. Qian, *Bioactive Materials*, 2022, **17**, 71-80.